ORIGINAL CONTRIBUTION

Dispersion of single-walled carbon nanotubes in aqueous solution with a thermo-responsive pentablock terpolymer

Yufeng Wu · Zanru Guo · Yujun Feng

Abstract Single-walled carbon nanotubes (SWNTs) were dispersed in pure water with a thermo-responsive amphiphilic PNIPAM$_{150}$-F108-PNIPAM$_{150}$ pentablock terpolymer in comparison with its precursor PEO$_{136}$-PPO$_{45}$-PEO$_{136}$ (F108) triblock copolymer. The stability, dispersibility, and thermo-responsive behaviors of the polymer/SWNT hybrids were characterized by UV–vis–NIR spectroscopy, thermal gravimetric analysis, viscosity measurement, Raman spectroscopy, and high-resolution transmission electron microscopy. The pentablock/SWNT hybrids showed superior ability in stabilization over F108/SWNT hybrids, and no sign of sedimentation was found at room temperature for 6 weeks or even 2 months of storage. The pentablock terpolymer can efficiently disperse SWNTs into individual tubes or small bundles with average diameter of about 5 nm, and their chains were helically wrapped onto the nanotube surface, whereas the larger bundles of the nanotubes with sizes of 15–25 nm were observed in F108/SWNT hybrids. Moreover, the pentablock/SWNT hybrids switched reversibly between the well-exfoliated and the aggregated states when cyclically increasing and decreasing temperature.

Y. Wu · Z. Guo · Y. Feng (✉)
Chengdu Institute of Organic Chemistry, Chinese Academy of Sciences, No. 9, Section 4, Renmin South Avenue, Chengdu 610041, People's Republic of China
e-mail: yjfeng@cioc.ac.cn

Y. Feng
Polymer Research Institute, State Key Laboratory of Polymer Materials Engineering, Sichuan University, Chengdu 610065, People's Republic of China

Y. Wu · Z. Guo
University of Chinese Academy of Sciences, Yuquan Road, Beijing 100039, People's Republic of China

Introduction

Since their discovery in 1993 [1], single-walled carbon nanotubes (SWNTs) have attracted great interdisciplinary interest due to their extraordinary optical, thermal, mechanical, and electronic properties [2–5]. Their versatile properties furnish them a wide scope of prospective applications, such as electronics [6, 7], sensors [8, 9], composite fibers [10–12], and medicinal materials [13–15]. For the pursuit of these applications, a solution-based SWNT process would be exceptionally useful. However, SWNTs usually tend to form bundles and clusters owing to the high aspect ratios and the strong intertubular van der Waals interaction, leading to their notoriously poor solubility and dispersibility in most solvents, especially in pure water, and thus severely impeding their further processing and end uses [10, 16]. To overcome these vital deficiencies, two main strategies have been developed in recent years: covalent functionalization of SWNTs with solvophilic molecules [17–22] and non-covalent surface coating by amphiphilic molecules [23–27]. The covalent method can notably improve the dispersion efficiency and solubility of SWNTs. Unfortunately, the covalent functionalization, typically carboxylation of the nanotubes, usually requires reaction under strong acidic conditions [20]. Thus, this procedure would inevitably destroy the electron conjugation system and create defects in the nanotube lattice, which can reduce their thermal and electrical conductivity and compromise their mechanical properties [10].

Compared to the covalent procedure, non-covalent interactions show the advantage of no disruption of the intrinsic structure, and thus, they can preserve the inherent properties and integrity of SWNTs [9]. It has been reported that surfactants [28, 29], polymers [24, 30, 31], as well as small molecules [9, 32] can disperse and improve the solubility of SWNTs in water through physical wrapping or encapsulation. In comparison with other functionalizing agents for SWNTs, amphiphilic block polymers [11, 33, 34] display superior dispersibility and solubility because their hydrophobic parts are oriented toward

the surface of nanotubes while their hydrophilic parts extend into solvents and prevent nanotubes from aggregating. Park and coauthors [34] dispersed SWNTs in various organic solvents using amphiphilic polystyrene-*b*-poly(4-vinylpyridine) diblock copolymer and found that the stability is superior to that by either surfactants or high molecular weight homopolymers, and no precipitation was observed after a 2-month standing. They also demonstrated that the block copolymer micelles are physically adsorbed onto the surface of SWNTs and thus hindered their aggregation. In addition, the amphiphilic Pluronic (PEO-PPO-PEO) triblock copolymers were also reported good candidates for dispersing SWNTs in aqueous solutions for bio-related applications [29, 35–39].

On the other hand, in many potential applications such as SWNT-based switching sensors, drug and gene delivery systems, it is highly desirable for controlling the dispersion and aggregation states of SWNTs in solvents with external stimuli [30, 40–44], and the earlier reports showed that the resulting SWNTs are not only dispersible but also well controlled by environmental stimuli. However, few attempts [44–46] have been made so far to tune the dispersion of SWNTs using thermo-responsive polymers through the non-covalent method. Although poly(*N*-isopropylacrylamide) (PNIPAM) is a well-known thermo-responsive polymer with LCST close to human body temperature [47], it has only modest physical affinity to the nanotubes, which is insufficient to stabilize and disperse nanotubes in pure water [44]. In this respect, incorporation of an amphiphilic component to PNIPAM would be a possible way to improve its affinity to the nanotubes without affecting its thermo-responsive behavior.

In a previous work [48], we have synthesized a series of thermo-responsive amphiphilic pentablock terpolymers, poly(*N*-isopropylacrylamide)-*b*-poly(ethylene oxide)-*b*-poly(propylene oxide)-*b*-poly(ethylene oxide)-*b*-poly(*N*-isopropylacrylamide). Here, one of such pentablock terpolymers, $PNIPAM_{150}$-PEO_{136}-PPO_{45}-PEO_{136}-$PNIPAM_{150}$, was chosen to disperse SWNTs in water. To better clarify the effect of different molecular structures on dispersibility and thermo-responsive properties, its triblock precursor, the commercially available PEO_{136}-PPO_{45}-PEO_{136} (F108) copolymer, was also examined for comparison.

Experimental

Materials

SWNTs (purity >90 %; OD 1–2 nm; length 5–30 μm) prepared by chemical vapor deposition (CVD) procedure were kindly provided by Timesnano (Chengdu, China) and used without further treatment. Pluronic F108 (PEO_{136}-PPO_{45}-PEO_{136}, $M_n = 1.46 \times 10^4$ g mol^{-1}) was purchased from Sigma-Aldrich and used without further purification. The

pentablock terpolymer, $PNIPAM_{150}$-PEO_{136}-PPO_{45}-PEO_{136}-$PNIPAM_{150}$ ($M_n = 4.91 \times 10^4$ g mol^{-1}, PDI=1.23) was synthesized and characterized as previously reported [48]. Their molecular structures are shown in Fig. 1. Other chemicals with the highest grade of purity were used as received, and water used was doubly distilled.

Sample preparation

Stock aqueous solutions were obtained by dissolving 0.1 g F108 or $PNIPAM_{150}$-F108-$PNIPAM_{150}$ in 5 mL deionized water, respectively. The mixtures were stored for 24 h at room temperature to get homogeneous polymer solutions. Then, 5.0 mg of SWNTs was added into the 5-mL polymer solutions, followed by sonication (KQ-100, Kunshan Ultrasound Instrument Company, China) at 100 W and 40 kHz for 1 h at room temperature. The resulting suspensions were centrifuged at 4,000 rpm for 10 min to give the homogeneous polymer/SWNT hybrids. After removing the supernatant, we found 0.5 mg of insoluble precipitate left. Deducting such insoluble precipitate, actually ca. 4.5 mg of SWNTs that was dispersed in water, i.e., the supernatants contain 0.1 g polymer and 4.5 mg of SWNTs. Such supernatants were stored at room temperature prior to further measurements.

Characterizations

UV–vis–NIR measurements were carried out on a computer-manipulated dual-beam spectrometer (UV–vis 4100, Hitachi, Japan) operated at a resolution of 1 nm at 25 and 50 °C, respectively. According to the previously reported measurement [30, 49], the absorbance in the wavelength range of 400–1,600 nm was recorded. However, the wavelength range of 400–1,300 nm was finally selected because the absorbance intensity of UV–vis–NIR spectra of our polymer/SWNT hybrids at a wavelength higher than 1,300 nm was beyond the measurement range of the instrument. The polymer/SWNT hybrids were diluted four-fold with deionized water prior to measurements, and the pure polymer aqueous solutions were used to get the baselines in corresponding measurements, respectively.

A Tecnai G2 F20 S-TWIN high-resolution transmission electron microscope (HR-TEM, FEI Co. Ltd., USA) equipped with a Schottky field emission gun at an accelerating voltage of 200 kV was used to characterize the dispersion of both hybrids. A drop of preheated (25 or 50 °C) supernatant was placed on ultrathin carbon-coated copper grids and dried in the oven for half an hour prior to observation.

Viscosity of the hybrids as a function of shear rate was measured using a Physica MCR 301 (Anton Paar, Austria) rotational rheometer equipped with concentric cylinder geometry CC27 (ISO3219). The rheometer was equipped with a Peltier temperature system that allows accurate control of temperature within ±0.01 °C. A solvent trap was used to
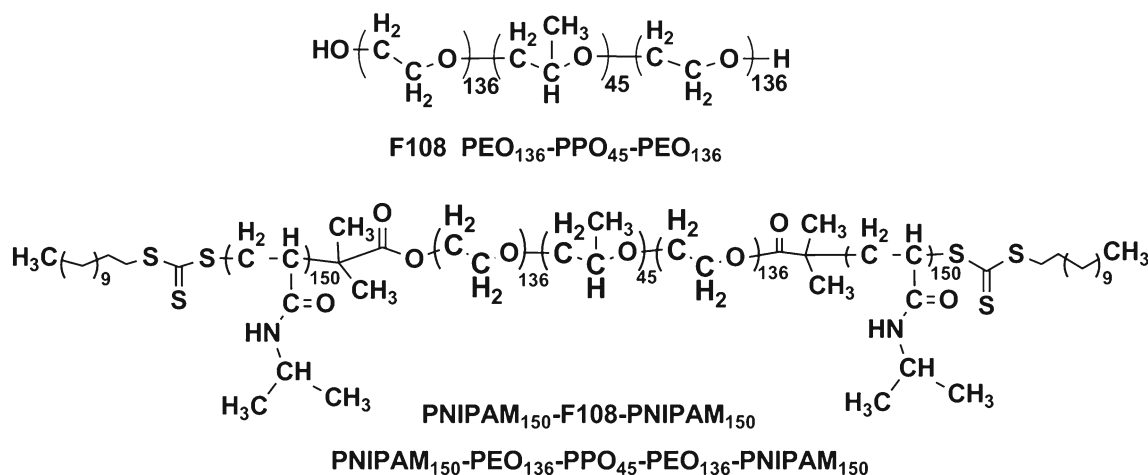
Fig. 1 The molecular structures of triblock copolymer (F108) and pentablock terpolymer (PNIPAM$_{150}$-F108-PNIPAM$_{150}$)

minimize changes in concentration due to water evaporation during the measurements.

Thermal gravimetric analysis (TGA) was conducted on a 299-F1 thermal analysis system (TA Instruments Q500), scanning from 15 to 600 °C at 10 °C min^{-1} under nitrogen atmosphere.

Raman spectra were registered on a LabRAM-HR Raman spectrometer (HORIBA Co., Ltd., France) using He–Ne laser as the light source at 785 nm. To gain the hybrids for TGA and Raman spectra analysis, the supernatants were filtered through a PTFE microporous membrane (220 nm), and the polymer/SWNT hybrids left on the membrane were then washed by deionized water and freeze-dried for 24 h before measurements.

Results and discussion

Dispersion of polymer/SWNT hybrids

The thermo-responsive behaviors of F108 copolymer and PNIPAM$_{150}$-F108-PNIPAM$_{150}$ pentablock terpolymer in aqueous solutions were thoroughly examined previously [48], and it was found that the pentablock terpolymer exhibited thermo-induced phase transition while no such behavior was found in F108 in the existing experimental conditions and the transition temperatures for pentablock terpolymer and F108 solutions were 35 and above 100 °C at 20 mg mL^{-1}, respectively. To check if such phase-transition behavior still exists in both F108/SWNT and pentablock/SWNT hybrids, we firstly made naked-eye observation on the resulting suspensions at 25 and 50 °C (Fig. 2), respectively. As we know, the visual observation was frequently employed to determine the dispersion of the nanotubes in solvents [33, 44]. The F108/SWNT hybrids are homogeneous with no visible sedimentation and present a stable black solution at 25 °C for 2 weeks of storage (Fig. 2a), but partial sedimentation of the nanotubes is evidenced after 3 weeks.

When the temperature was increased to 50 °C, still no obvious thermo-induced phase transition is witnessed (Fig. 2b). Similar to F108/SWNT hybrids, the pentablock/SWNT hybrids are also completely dispersed with a stable black solution for 6 weeks or even 2 months of storage at 25 °C (Fig. 2c) because the terpolymer chains are fully dissolved and able to interact with the nanotubes. However, when the temperature increased up to 50 °C (Fig. 2d), the SWNTs settled down in water due to the shrinkage and collapse of the terpolymer chains. As the temperature decreased again to 25 °C (Fig. 2e), the hybrids are re-dispersed with a homogeneous black solution due to the re-extension of the terpolymer chains. Thus, the dispersion/aggregation states of pentablock/SWNT hybrids can be reversibly switched by temperature stimulus.

In parallel with the visual observation, HR-TEM, a well-established technique for observing the microstructures of the nanotubes [5], was conducted to further get more accurate thermal-responsive dispersion/aggregation information of the polymer/SWNT hybrids. Presented in Fig. 3 are the HR-TEM images of pentablock/SWNT and F108/SWNT hybrids in water at 25 and 50 °C, respectively. As shown in Fig. 3a, the pentablock/SWNT hybrids are well exfoliated with individual ones or small bundle tubes. So that the dispersion of SWNTs can be observed more clearly, the higher magnifications for the pentablock/SWNT hybrids are displayed in Fig. 3b. It can be seen that the small bulges on the sidewall of the nanotubes are ascribed to the helical wrapping of pentablock terpolymer chains. As is well known, SWNTs usually tend to form large bundles and ropes due to the strong intertubular van der Waals interaction; however, the nanotubes coated with pentablock terpolymer dispersed uniformly and individually rather than ropes. The observed diameters of the dispersed nanotubes are about 5 nm, three times larger than that of the pristine tubes, indicating that the nanotubes are surrounded by a thick polymer layer. Nevertheless, when the temperature is increased to 50 °C, the hybrids exhibit a heavily bundled and networked
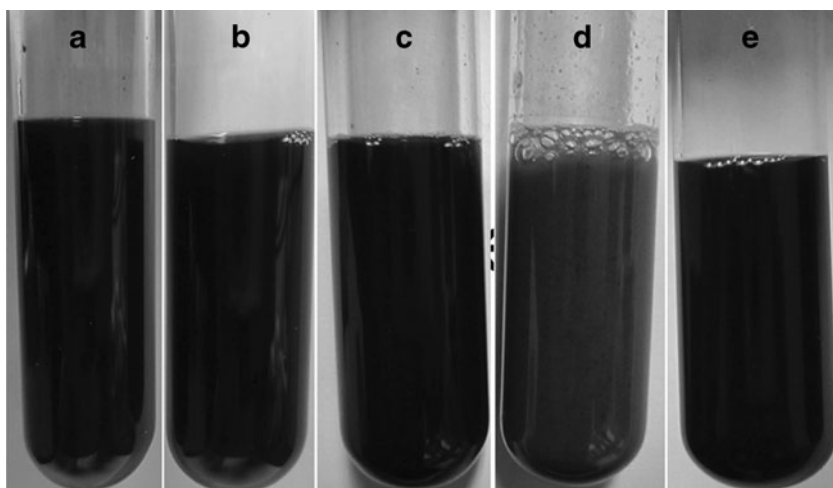
microstructure (Fig. 3c). These results suggest that the intermolecular hydrogen bonding between the polymers and water molecules is predominant at low temperature, and the terpolymer chains are extended and soluble in water, leading to SWNTs being soluble in water. However, at high temperature, the intramolecular hydrogen bonding between C=O and N–H groups and stronger hydrophobic attraction forces of PPO groups result in a compact and collapsed conformation

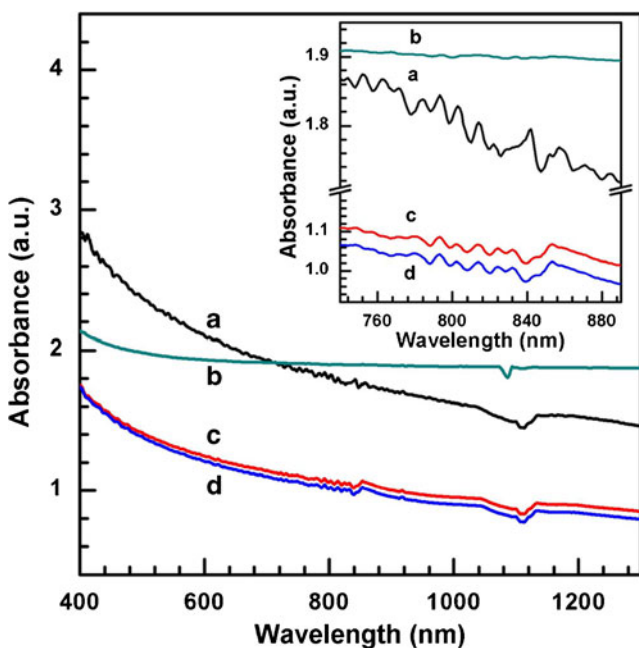of the terpolymer chains, which makes SWNTs difficult to be soluble in water [50, 51].

In regard to the dispersion of SWNTs by F108, much larger bundles (15–25 nm) are observed (Fig. 3d), suggestive of poor exfoliation of the nanotubes. At 50 °C, the crowded and larger bundled SWNTs are also clearly observed (Fig. 3e), which has similar morphology as appears in Fig. 3d, implying that the influence of temperature on F108/SWNT hybrids is negligible.
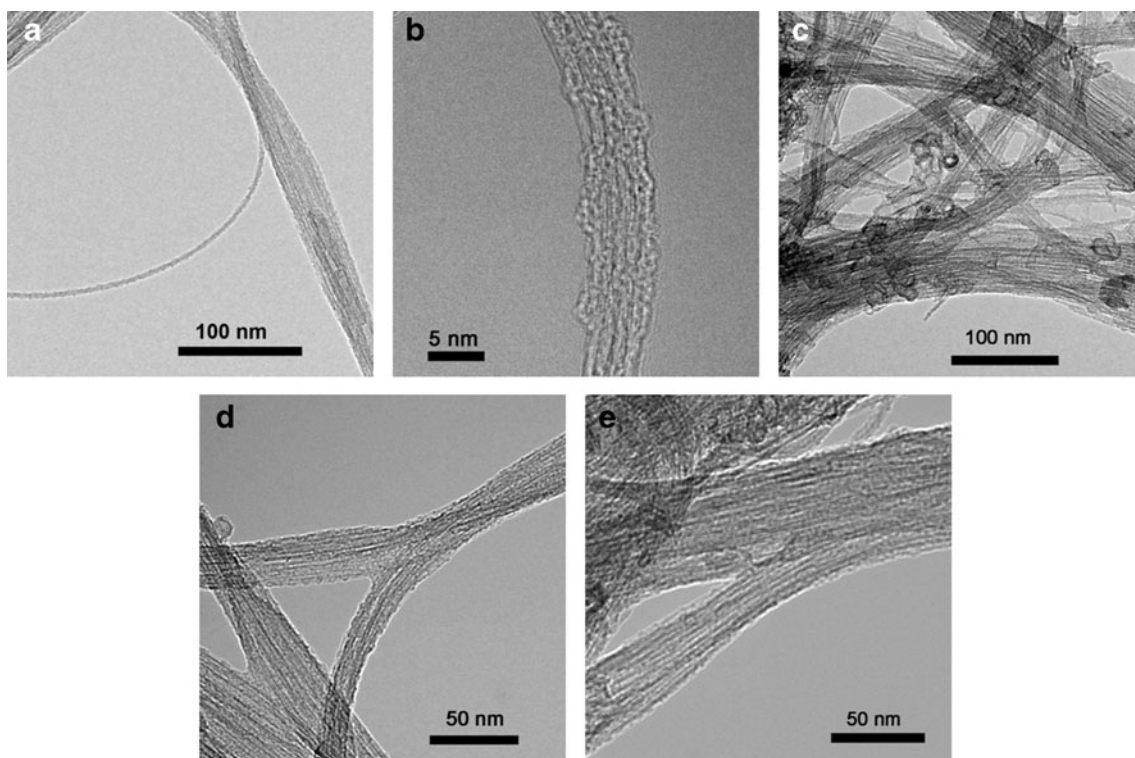
Fig. 3 HR-TEM images of pentablock/SWNT hybrids in water at 25 (**a**, **b**) and 50 °C (**c**), and F108/SWNT hybrids in water at 25 (**d**) and 50 °C (**e**), respectively

This is in accordance with the macroscopic observation as described above.

In order to better interpret the effect of temperature on the dispersion state, UV–vis–NIR spectroscopy, a well-recognized useful technique for characterizing the nanotubes [21, 52], was employed to monitor the variation of the absorbance of both the hybrids. Displayed in Fig. 4 are the UV–vis–NIR absorption spectra of the pentablock/SWNT and F108/SWNT hybrids in water at 25 and 50 °C, respectively. It was found that the strong absorptions with several sharp peaks located in the region of 750–890 nm are observed at 25 °C for pentablock/SWNT hybrids (Fig. 4, curve a), implying a favorable dispersion ability of the nanotubes. However, at 50 °C (Fig. 4, curve b), the characteristic peaks of pentablock/SWNT hybrids completely disappeared, indicating that the bundled nanotubes are re-formed. As displayed in curves c and d of Fig. 4, the several sharp peaks in the region of 750–890 nm are also observed for F108/SWNT hybrids, and the absorption intensity at 25 °C has similar values to that at 50 °C, suggesting the dispersing ability is not influenced by temperature. It should be noted that the average spectroscopic features of SWNTs are observed because their diameter and helicity are polydispersed, especially those prepared by CVD procedure [16, 53], just like the SWNTs used in this work, and the characteristic absorption bands (750–890 nm) are corresponding to the absorption features of the van Hove transition semiconducting tubes, indicative of the well-exfoliated SWNTs [21].
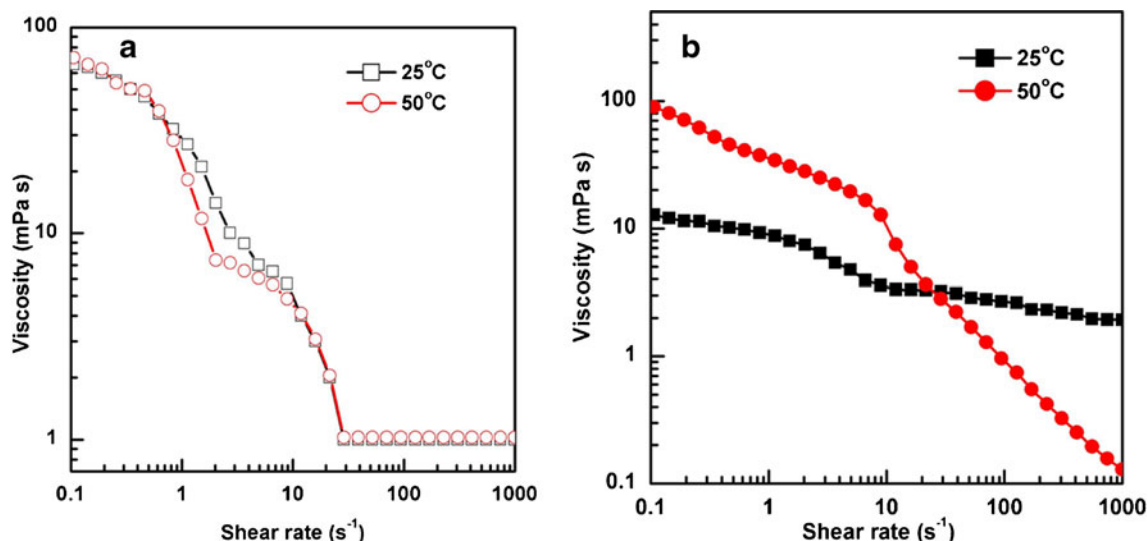
So that the typical absorption of SWNTs is observed more clearly, the absorption intensities in the 750–890-nm regions for both the hybrids are magnified and inserted into Fig. 4. One can find that the pentablock/SWNT hybrids (the inset curve a) show well-resolved absorption peaks compared to the F108/SWNT hybrids (the inset curve c) at 25 °C, and the absorbance intensity of the former hybrids is ca. twice as high as that of the latter case. As reported previously [30, 54], the sharpness of absorption peaks reflects the level of isolation of the nanotubes, and the absorption intensity is proportional to the amount of dispersed nanotubes, independent of whether they are isolated or bundled. Thus, these results reveal that more effective exfoliation of SWNTs is achieved by the pentablock terpolymer than F108 at low temperature; in other words, the pentablock terpolymer is superior to F108 in dispersing SWNTs. This may result from the incorporation of PNIPAM groups in pentablock terpolymer, which enhances the hydrophobic interaction between the terpolymer chains and the nanotubes [55].

Meanwhile, in an effort to further investigate the thermo-responsive behaviors, viscosity measurements were also made on the F108/SWNT and pentablock/SWNT hybrids. Figure 5 shows the viscosity as a function of shear rate for the two hybrids at 25 and 50 °C, respectively. It was found that the F108/SWNT hybrids show shear-thinning behavior (i.e., decreasing viscosity with increasing shear rate) at 25 and 50 °C, respectively, suggesting bundled nanotube microstructure without a temperature-responsive behavior [56]. However, the pentablock/SWNT hybrids display a nearly Newtonian behavior with little change in viscosity as a function of shear rate at 25 °C and shear-thinning behavior at 50 °C, respectively, suggesting a thermo-responsive behavior [46].

To better understand how the polymer chains attached onto SWNTs, Raman spectroscopy, which offers a great deal of useful information concerning modification of SWNTs, was employed. Typical Raman spectra of SWNTs exhibit three main characteristic Raman modes: the diameter-dependent radial breathing modes (RBM, frequency 100–300 cm^{-1}), the disorder mode (D, −1,350 cm^{-1}), and the tangential mode (G, −1,580 cm^{-1}). The RBM peaks are highly sensitive to the diameter but not the helicity of nanotubes; the D mode is related to the amount of disordered graphite, and the G mode is referred to the tangential C–C stretching vibrations [57].

Figure 6 shows the Raman spectra of the pristine SWNTs and the F108/SWNT and pentablock/SWNT hybrids, respectively. The RBM peaks for original SWNTs with positions of about 156 and 267 cm^{-1}, which correspond to a mean diameter of 1.43 and 0.84 nm, respectively, according to the well-known relation between the

Fig. 4 UV–vis–NIR absorption spectra of pentablock/SWNT hybrids in water at 25 (**a**) and 50 °C (**b**) and F108/SWNT hybrids in water at 25 (**c**) and 50 °C (**d**), respectively. The polymer concentration is 5 mg mL^{-1}, and the concentration of SWNTs is 0.225 mg mL^{-1}

Fig. 5 Viscosity as a function of shear rate for F108/SWNT hybrids (**a**) and pentablock/SWNT hybrids (**b**) at 25 and 50 °C, respectively

RBM band frequency and the diameter $d=223.75/RBM$ [57]. The D peak of the pristine SWNTs can be found at 1,310 cm^{-1}, and its G mode is located around 1,581 cm^{-1}. Here, three mode positions of the original SWNTs are used to compare with those of both hybrids. As shown in Fig. 6a, the intensity and sharpness of the D modes of both hybrids have changed somewhat in contrast to those of the pristine SWNTs, while the spectral shift is insignificant, indicating that the non-covalent modification and the sonication condition in our experiments do not cause obvious destruction on the nanotubes [33]. The profile and peak positions of RBM and G modes of both hybrids shift to higher frequencies compared to those of the original SWNTs, and the amplified changes are displayed in Fig. 6b and c, respectively. The RBM peaks of F108/SWNT hybrids are located at 159 and 267 cm^{-1}, and the corresponding peaks of pentablock/

SWNT hybrids are observed at 160 and 267 cm^{-1} (Fig. 6b), respectively. In contrast with the RBM peak positions of the pristine SWNTs, one can find that only the RBM peak located at 156 cm^{-1} upshifts to 159 and 160 cm^{-1}, respectively, indicating a reduction in the diameter and debundled process of the nanotubes [26]. However, another RBM peak located at 267 cm^{-1} has not been changed, implying that the polymer matrix selectively disperses SWNTs with a certain diameter, which is 1.43 nm in our case. In addition, a clear trend in the spectral position of the G mode can also be observed (Fig. 6c), and the G peaks of F108/SWNT and pentablock/SWNT hybrids are located at 1,585 and 1,586 cm^{-1}, respectively. Taking into account the peak at 1,581 cm^{-1} of the pristine SWNTs, their G peaks are seen to shift to higher frequency 4–5 cm^{-1}. This result can be explained by considering helical
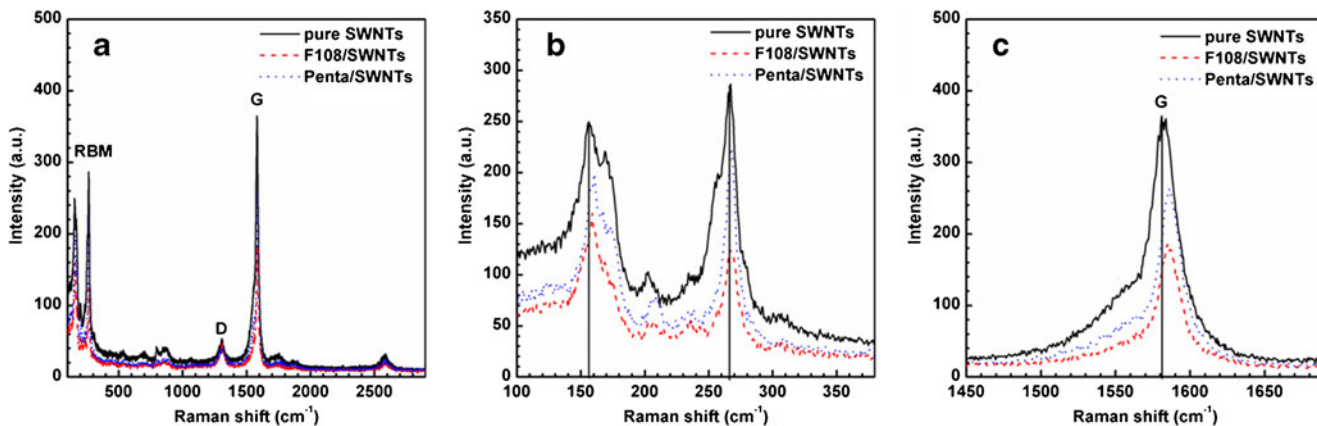

Fig. 6 a Raman spectroscopy of pristine SWNTs, F108/SWNT, and pentablock/SWNT, **b** the magnified radial breathing modes, and **c** the magnified tangential mode

wrapping and the stronger hydrophobic attraction forces between the polymer chains and the nanotubes [33, 58].

Polymers wrapped onto the surface of SWNTs

TGA analysis was performed on the resulting hybrids in order to obtain the relative amounts of F108 and pentablock terpolymer wrapped on SWNTs. Figure 7 compares the TGA results of the pristine SWNTs, F108, F108/ SWNT, pentablock terpolymer, and pentablock/SWNT, respectively. It can be seen that the pristine SWNTs start to decompose at around 500 °C, and the approximately 4 wt% mass loss of polymers and polymer/SWNT hybrids is observed in the region of 15–185 °C, which can be attributed to the minor amount of adsorbed water in both hybrids. Compared to the TGA profile of F108, the major decomposition of F108/SWNT hybrids occurred in the temperature range 200–450 °C corresponding to the wrapped F108 on the surface of the nanotubes, and the weight percentage of F108 in hybrids is ca. 14.2 wt%. Similarly, the pentablock terpolymer is completely decomposed at about 450 °C, from which we can get that the weight percentage in pentablock/SWNT hybrids is about 43.8 wt%. The result shows that the amount of pentablock terpolymer wrapped on the nanotubes is significantly greater than that of F108. It should be noted that 4.5 mg SWNTs and 100 mg polymers are dispersed in 5 mL supernatant; that is, the weight percentage of polymers attached onto the nanotubes is about 95.7 wt%.
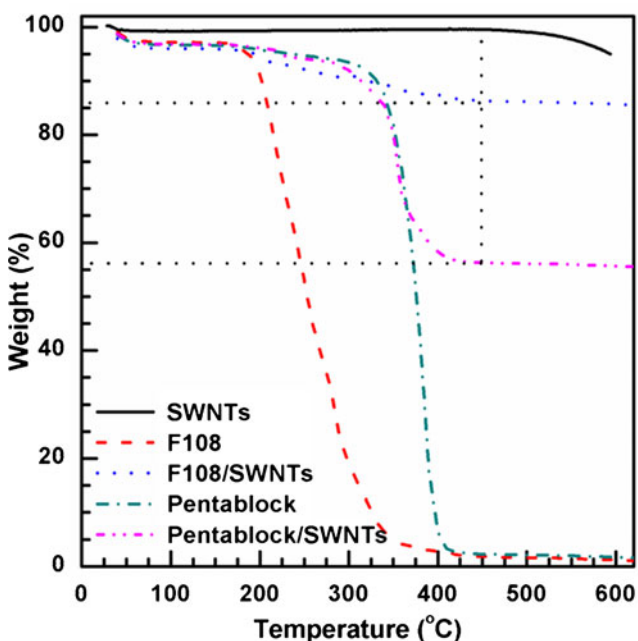
Nevertheless, TGA results show that the weight percentages of polymer are only 14.2 and 43.8 wt% in both hybrids, respectively. The polymer contents in hybrids determined by TGA are much lower than the calculated loading, implying that there is either equilibrium between the bound and excess polymer, or an excess of polymer is somehow needed to support SWNTs to be dispersed in water [31].

According to the above TGA results, one can calculate the average number of polymer chains attached onto SWNTs. First, we presume that the polymer/SWNT hybrids are 1.0 g. Based on the TGA analyses, the weights of pentablock terpolymer ($W_{polymer}$) and SWNTs (W_{SWNTs}) are 0.438 and 0.562 g, respectively. The average molecular weight of our SWNTs (length 10 μm; diameter 1.2 nm) is about 17,300,000 g mol^{-1} [42]. Then, the average number (z) of polymer chains attached onto one nanotube can be calculated from

$$z = \frac{\dfrac{W_{polymer}}{M_{n(polymer)}} \times N_A}{\dfrac{W_{SWNTs}}{M_{n(nanotube)}} \times N_A} \tag{1}$$

where N_A is Avogadro's number. The z is calculated to be 275 for pentablock/SWNT hybrids. That is to say, one nanotube is wrapped with roughly 275 pentablock terpolymer chains. Similarly, one carbon nanotube is wrapped with approximately 196 triblock copolymer chains. It is worth emphasizing that such a calculation is just an estimation because we cannot get the SWNTs with uniform length [42].

Conclusions

The stability, dispersibility, and thermo-responsive behaviors of SWNTs dispersed by pentablock terpolymer and F108 were investigated. The pentablock/SWNT hybrids showed superior dispersion and stability in pure water over the F108/SWNT hybrids, and the individual tubes or small bundles were observed in the former case, while large bundle tubes were presented in the latter system. The pentablock terpolymer chains were helically wrapped onto the surface of SWNTs. The diameters of SWNTs were reduced after dispersion by polymers due to the stronger hydrophobic attraction forces between the polymer chains and the nanotubes. The pentablock/SWNT hybrids exhibited switchable dispersion/aggregation states upon temperature stimulus. Such a kind of thermo-switchable hybrids may find potential applications in sensor of biomedicines or drug and gene delivery.

Fig. 7 TGA traces for pristine SWNTs, F108, F108/SWNT, pentablock terpolymer, and pentablock/SWNT, respectively

References

1. Iijima S, Ichihashi T (1993) Single-shell carbon nanotubes of 1-nm diameter. Nature 363:603–605
2. Chen J, Hamon MA, Hu H, Chen YS, Rao AM, Eklund PC, Haddon RC (1998) Solution properties of single-walled carbon nanotubes. Science 282:95–98
3. Kharisov BI, Kharissova OV, Gutierrez HL, Mendez UO (2009) Recent advances on the soluble carbon nanotubes. Ind Eng Chem Res 48:572–590
4. Spitalsky Z, Tasis D, Papagelis K, Galiotis C (2010) Carbon nanotube–polymer composites: chemistry, processing, mechanical and electrical properties. Prog Polym Sci 35:357–401
5. Ajayan PM (1999) Nanotubes from carbon. Chem Rev 99:1787–1799
6. Ajayan PM, Charlier JC, Rinzler AG (1999) Carbon nanotubes: from macromolecules to nanotechnology. Proc Natl Acad Sci USA 96:14199–14200
7. Baughman RH, Zakhidov AA, de Heer WA (2002) Carbon nanotubes—the route toward applications. Science 297:787–792
8. Dai HJ (2002) Carbon nanotubes: synthesis, integration, and properties. Acc Chem Res 35:1035–1044
9. Chen RJ, Bangsaruntip S, Drouvalakis KA, Kam NWS, Shim M, Li YM, Kim W, Utz PJ, Dai HJ (2003) Noncovalent functionalization of carbon nanotubes for highly specific electronic biosensors. Proc Natl Acad Sci USA 100:4984–4989
10. Ajayan PM, Tour JM (2007) Materials science—nanotube composites. Nature 447:1066–1068
11. Szleifer I, Yerushalmi-Rozen R (2005) Polymers and carbon nanotubes—dimensionality, interactions and nanotechnology. Polymer 46:7803–7818
12. Andrews R, Weisenberger MC (2004) Carbon nanotube polymer composites. Curr Opin Solid St M 8:31–37
13. Liu C, Fan YY, Liu M, Cong HT, Cheng HM, Dresselhaus MS (1999) Hydrogen storage in single-walled carbon nanotubes at room temperature. Science 286:1127–1129
14. Wang ZH, Wang YM, Luo G (2002) A selective voltammetric method for uric acid detection at beta-cyclodextrin modified electrode incorporating carbon nanotubes. Analyst 127:1353–1358
15. Liu Z, Chen K, Davis C, Sherlock S, Cao QZ, Chen XY, Dai HJ (2008) Drug delivery with carbon nanotubes for in vivo cancer treatment. Cancer Res 68:6652–6660
16. Tasis D, Tagmatarchis N, Georgakilas V, Prato M (2003) Soluble carbon nanotubes. Chem Eur J 9:4001–4008
17. Homenick CM, Lawson G, Adronov A (2007) Polymer grafting of carbon nanotubes using living free-radical polymerization. Polym Rev 47:265–290
18. Viswanathan G, Chakrapani N, Yang HC, Wei BQ, Chung HS, Cho KW, Ryu CY, Ajayan PM (2003) Single-step in situ synthesis of polymer-grafted single-wall nanotube composites. J Am Chem Soc 125:9258–9259
19. Bahr JL, Yang JP, Kosynkin DV, Bronikowski MJ, Smalley RE, Tour JM (2001) Functionalization of carbon nanotubes by electrochemical reduction of aryl diazonium salts: a bucky paper electrode. J Am Chem Soc 123:6536–6542
20. Hirsch A (2002) Functionalization of single-walled carbon nanotubes. Angew Chem Int Ed 41:1853–1859
21. Strano MS, Dyke CA, Usrey ML, Barone PW, Allen MJ, Shan HW, Kittrell C, Hauge RH, Tour JM, Smalley RE (2003) Electronic structure control of single-walled carbon nanotube functionalization. Science 301:1519–1522
22. Su X, Shuai Y, Guo ZR, Feng YJ (2013) Functionalization of multi-walled carbon nanotubes with thermo-responsive azide-terminated poly(N-isopropylacrylamide) via click reactions. Molecules 18:4599–4612
23. Lee JU, Huh J, Kim KH, Park C, Jo WH (2007) Aqueous suspension of carbon nanotubes via non-covalent functionalization with oligothiophene-terminated poly(ethylene glycol). Carbon 45:1051–1057
24. Kang YK, Lee OS, Deria P, Kim SH, Park TH, Bonnell DA, Saven JG, Therien MJ (2009) Helical wrapping of single-walled carbon nanotubes by water soluble poly(p-phenyleneethynylene). Nano Lett 9:1414–1418
25. Rungrotmongkol T, Arsawang U, Iamsamai C, Vongachariya A, Dubas ST, Ruktanonchai U, Soottitantawat A, Hannongbua S (2011) Increased dispersion and solubility of carbon nanotubes noncovalently modified by the polysaccharide biopolymer, chitosan: MD simulations. Chem Phys Lett 507:134–137
26. Hu CG, Chen ZL, Shen AG, Shen XC, Li H, Hu SS (2006) Water-soluble single-walled carbon nanotubes via noncovalent functionalization by a rigid, planar and conjugated diazo dye. Carbon 44:428–434
27. Xin X, Xu GY, Zhao TT, Zhu YY, Shi XF, Gong HJ, Zhang ZQ (2008) Dispersing carbon nanotubes in aqueous solutions by a star-like block copolymer. J Phys Chem C 112:16377–16384
28. Vaisman L, Wagner HD, Marom G (2006) The role of surfactants in dispersion of carbon nanotubes. Adv Colloid Interface Sci 128:37–46
29. Monteiro-Riviere NA, Inman AO, Wang YY, Nemanich RJ (2005) Surfactant effects on carbon nanotube interactions with human keratinocytes. Nanomedicine-Nanotechnol 1:293–299
30. Umeyama T, Kawabata K, Tezuka N, Matano Y, Miyato Y, Matsushige K, Tsujimoto M, Isoda S, Takano M, Imahori H (2010) Dispersion of carbon nanotubes by photo- and thermal-responsive polymers containing azobenzene unit in the backbone. Chem Commun 46:5969–5971
31. Star A, Stoddart JF, Steuerman D, Diehl M, Boukai A, Wong EW, Yang X, Chung SW, Choi H, Heath JR (2001) Preparation and properties of polymer-wrapped single-walled carbon nanotubes. Angew Chem Int Ed 40:1721–1725
32. Liu Z, Davis C, Cai WB, He L, Chen XY, Dai HJ (2008) Circulation and long-term fate of functionalized, biocompatible single-walled carbon nanotubes in mice probed by Raman spectroscopy. Proc Natl Acad Sci USA 105:1410–1415
33. Sinani VA, Gheith MK, Yaroslavov AA, Rakhnyanskaya AA, Sun K, Mamedov AA, Wicksted JP, Kotov NA (2005) Aqueous dispersions of single-wall and multiwall carbon nanotubes with designed amphiphilic polycations. J Am Chem Soc 127:3463–3472
34. Shin HI, Min BG, Jeong WY, Park CM (2005) Amphiphilic block copolymer micelles: new dispersant for single wall carbon nanotubes. Macromol Rapid Commun 26:1451–1457
35. Alexandridis P, Hatton TA (1995) Poly(ethylene oxide)–poly(propylene oxide)–poly(ethylene oxide) block copolymer surfactants in aqueous solutions and at interfaces: thermodynamics, structure, dynamics, and modeling. Colloid Surf 96:1–46
36. Moore VC, Strano MS, Haroz EH, Hauge RH, Smalley RE, Schmidt J, Talmon Y (2003) Individually suspended single-walled carbon nanotubes in various surfactants. Nano Lett 3:1379–1382
37. Bardi G, Vittorio O, Maffei M, Pizzorusso T, Costa M (2009) Adipocytes differentiation in the presence of Pluronic F127-coated carbon nanotubes. Nanomedicine-Nanotechnol 5:378–381
38. Gong HJ, Xu GY, Liu T, Pang JY, Dou WL, Xin X (2011) Synthesis of block polyethers with various structures and their application in dispersing single-walled carbon nanotubes. Colloid Polym Sci 289:933–942
39. Pang JY, Xu GY, Tan YB, He F (2010) Water-dispersible carbon nanotubes from a mixture of an ethoxy-modified trisiloxane and pluronic block copolymer F127. Colloid Polym Sci 288:1665–1675

40. Barone PW, Strano MS (2006) Reversible control of carbon nanotube aggregation for a glucose affinity sensor. Angew Chem Int Ed 45:8138–8141

41. Doe C, Jang HS, Kim TH, Kline SR, Choi SM (2009) Thermally switchable one- and two-dimensional arrays of single-walled carbon nanotubes in a polymeric system. J Am Chem Soc 131:16568–16572

42. Guo ZR, Feng YJ, He S, Qu MZ, Chen HL, Liu HB, Wu YF, Wang Y (2013) CO_2-responsive "smart" single-walled carbon nanotubes. Adv Mater 25:584–590

43. Guo ZR, Feng YJ, Zhu DW, He S, Liu HB, Shi XR, Sun J, Qu MZ (2013) Light-switchable single-walled carbon nanotubes based on host-guest chemistry. Adv Funct Mater. doi:10.1002/adfm.201300434

44. Wang D, Chen LW (2007) Temperature and pH-responsive single-walled carbon nanotube dispersions. Nano Lett 7:1480–1484

45. Etika KC, Jochum FD, Theato P, Grunlan JC (2009) Temperature controlled dispersion of carbon nanotubes in water with pyrene-functionalized poly(N-cyclopropylacrylamide). J Am Chem Soc 131:13598–13599

46. Etika KC, Jochum FD, Cox MA, Schattling P, Theato P, Grunlan JC (2010) Nanotube friendly poly(N-isopropylacrylamide). Macromol Rapid Commun 31:1368–1372

47. Schild HG (1992) Poly(N-isopropylacrylamide): experiment, theory and application. Prog Polym Sci 17:163–249

48. Wu YF, Liu XL, Wang Y, Guo ZR, Feng YJ (2012) Synthesis and aggregation behaviors of well-defined thermo-responsive pentablock terpolymers with tunable LCST. Macromol Chem Phys 213:1489–1498

49. Hwang JY, Nish A, Doig J, Douven S, Chen CW, Chen LC, Nicholas RJ (2008) Polymer structure and solvent effects on the selective dispersion of single-walled carbon nanotubes. J Am Chem Soc 130:3543–3553

50. Hong CY, You YZ, Pan CY (2005) Synthesis of water-soluble multiwalled carbon nanotubes with grafted temperature-responsive shells by surface RAFT polymerization. Chem Mater 17:2247–2254

51. Zhang JP, Wang AQ (2009) pH- and thermo-responsive dispersion of single-walled carbon nanotubes modified with poly(N-isopropylacrylamide-co-acrylic acid). J Colloid Interface Sci 334:212–216

52. Pal A, Chhikara BS, Govindaraj A, Bhattacharya S, Rao CNR (2008) Synthesis and properties of novel nanocomposites made of single-walled carbon nanotubes and low molecular mass organogels and their thermo-responsive behavior triggered by near IR radiation. J Mater Chem 18:2593–2600

53. Kong J, Zhou C, Morpurgo A, Soh HT, Quate CF, Marcus C, Dai H (1999) Synthesis, integration, and electrical properties of individual single-walled carbon nanotubes. Appl Physiol A-Mater 69:305–308

54. O'Connell MJ, Bachilo SM, Huffman CB, Moore VC, Strano MS, Haroz EH, Rialon KL, Boul PJ, Noon WH, Kittrell C, Ma JP, Hauge RH, Weisman RB, Smalley RE (2002) Band gap fluorescence from individual single-walled carbon nanotubes. Science 297:593–596

55. Chen SL, Jiang YG, Wang ZQ, Zhang X, Dai LM, Smet M (2008) Light-controlled single-walled carbon nanotube dispersions in aqueous solution. Langmuir 24:9233–9236

56. Shaffer MSP, Windle AH (1999) Analogies between polymer solutions and carbon nanotube dispersions. Macromolecules 32:6864–6866

57. Saito R, Dresselhaus G, Dresselhaus MS (2000) Trigonal warping effect of carbon nanotubes. Phys Rev B 61:2981–2990

58. Chatterjee T, Yurekli K, Hadjiev VG, Krishnamoorti R (2005) Single-walled carbon nanotube dispersions in poly(ethylene oxide). Adv Funct Mater 15:1832–1838